

VIP Gas Separation Very Important Paper Hot Paper

 How to cite: *Angew. Chem. Int. Ed.* **2024**, e202419091
 doi.org/10.1002/anie.202419091

Molecular Trapdoor in HEU Zeolite Enables Inverse CO₂-C₂H₂ Separation

Jizhen Jia[†], Nana Yan[†], Xin Lian, Shanshan Liu,* Bin Yue, Yuchao Chai, Guangjun Wu, Jian Xu, and Landong Li*

Abstract: The adsorptive separation of molecules with very similar physical properties is always a challenging task. Reported herein is the design and tailoring of zeolite adsorbent for the precise discrimination and separation of CO₂-C₂H₂ mixture through the pronounced trapdoor effect. Typically, Sr exchanged K-type clinoptilolite, namely Sr/K-HEU, is developed as a robust zeolite adsorbent for inverse CO₂-C₂H₂ separation, showing the state-of-the-art dynamic CO₂/C₂H₂ selectivity of 48.0 and sustainable CO₂ dynamic uptake of 0.96 mmol/g at the same time. The perfect recyclability and the intrinsic low-cost nature of Sr/K-HEU make it a promising candidate for practical applications. Three-dimensional electron diffraction determines the precise structure of Sr/K-HEU and density functional theory calculations reveal the intricate interplay between guest molecules and the gate-keeping extraframework cations. Briefly, extraframework Sr²⁺ cations from the ten-membered rings of HEU zeolites act as the molecular trapdoor, allowing the entry of CO₂ molecules while excluding C₂H₂. This work presents a new example of molecular trapdoor in zeolite and its successful application in the challenging inverse CO₂-C₂H₂ separation, which not only expands the scope of molecular trapdoor concept but also improves current understanding on the nature of molecular trapdoor.

Introduction

Acetylene (C₂H₂) stands as an important industrial raw material, serving not merely as vital gas fuel, but more importantly as a key feedstock for the production of valuable chemicals and synthetic materials.^[1–3] C₂H₂ can be obtained from the partial combustion of natural gas and the steam cracking of hydrocarbons, with the co-production of a significant amount of carbon dioxide (CO₂).^[4,5] Consequently, the separation of CO₂ from C₂H₂ to secure high-purity C₂H₂ is an essential step for its downstream applications. Liquid extraction and cryogenic distillation are currently employed as the predominant technologies in industry to obtain high-purity C₂H₂ from the mixtures containing CO₂ and C₂H₂, which unfortunately suffer from substantial drawbacks such as huge energy consumption, high operating cost, and environmental unfriendliness.^[6,7] A surge of interest has arisen in the quest for more sustainable and cost-effective CO₂-C₂H₂ separation technologies. Therefore, the adsorptive separation emerges as a promising alternative, relying on the availability of adsorbents with high dynamic uptake and selectivity.^[8–10] The formidable challenges in the adsorptive separation of CO₂-C₂H₂ are obvious due to the molecular resemblance shared by CO₂ and C₂H₂, for example the kinetic diameter and physical properties including the boiling point, the dipole moment as well as the polarizability (Supporting Information, Table S1).^[6,7,11]

Various porous adsorbents have been explored for CO₂-C₂H₂ separation, and most of them preferentially trap C₂H₂ with moderate selectivity, owing to the slightly higher polarizability and quadrupole moment of C₂H₂.^[12–18] This necessitates further desorption processes to attain high-purity C₂H₂, thereby engendering a convoluted separation process and exacerbating energy wastage. In contrast, the allure of CO₂-selective adsorbents lies in their ability to facilitate the direct acquisition of high-purity C₂H₂ in a single step. However, the development of such CO₂-selective adsorbents is a very challenging task, and only a handful of metal-organic frameworks (MOFs) have been reported so far.^[19–25] The regulation of adsorption sites,^[26,27] control of pore environment,^[28–31] and kinetic-sieving^[21,32,33] have been proposed as available features to optimize CO₂ recognition by MOFs for inverse CO₂-C₂H₂ separation.

Zeolites have been widely used as industrial adsorbents for decades, showing unparalleled advantages of good stability, large-scale availability and low production cost.^[34–36] Adsorptive separation by zeolites is mainly based

[*] J. Jia,[†] Dr. S. Liu, B. Yue, Prof. Y. Chai, Prof. G. Wu, Prof. L. Li
 Key Laboratory of Advanced Energy Materials Chemistry of Ministry of Education, College of Chemistry,
 Nankai University,
 Tianjin 300071, P.R. China
 E-mail: liushanshan@nankai.edu.cn
 lild@nankai.edu.cn

J. Jia,[†] Dr. X. Lian, Dr. S. Liu, B. Yue, Prof. J. Xu
 School of Materials Science and Engineering,
 Nankai University,
 Tianjin 300350, P.R. China

Dr. N. Yan[†]
 National Engineering Research Center of Lower-Carbon Catalysis
 Technology, Dalian Institute of Chemical Physics, Chinese Academy
 of Sciences,
 Dalian 116023, P.R. China

Prof. L. Li
 Frontiers Science Center for New Organic Matter,
 Nankai University,
 Tianjin 300071, P.R. China

[†] Jizhen Jia and Nana Yan contributed equally to this work.

on physisorption and size-sieving, usually not applicable for the challenging $\text{CO}_2\text{-C}_2\text{H}_2$ separation. In fact, the efficient $\text{CO}_2\text{-C}_2\text{H}_2$ separation has only been achieved with Cu@FAU zeolite wherein C_2H_2 molecules are selectively trapped through reversible chemical bonding on coordinatively unsaturated Cu sites confined in zeolite.^[37] It seems very difficult to obtain a CO_2 -selective zeolite adsorbent for efficient $\text{CO}_2\text{-C}_2\text{H}_2$ separation considering the fact that the ubiquitous local electrostatic field within zeolites will exhibit stronger affinity toward C_2H_2 molecules with higher polarizability and larger quadrupole moment than CO_2 . On the other hand, the adsorption behaviors of guest molecules on zeolites show great diversity, among which an interesting mechanism, namely the trapdoor effect, a subset of the so-called gating flexibility, has been disclosed.^[38–41] Typically, the accessibility of the guest molecules to the internal cavities is determined by their ability of inducing temporary and reversible cation deviation to open the door for entering.^[42] This mechanism usually occurs in small-pore zeolites with eight-membered rings (8MRs) windows and large gate-keeping cations (K^+ and Cs^+), by which efficient $\text{CO}_2\text{-CH}_4$ and $\text{CH}_4\text{-N}_2$ separations have been achieved.^[43–45] The trapdoor effect by zeolites may offer new opportunities for the challenging inverse $\text{CO}_2\text{-C}_2\text{H}_2$ separation.

Herein, the trapdoor effect by Sr-exchanged K-type clinoptilolite (Sr/K-HEU) zeolite is disclosed for the first time and successfully applied in the inverse $\text{CO}_2\text{-C}_2\text{H}_2$ separation. Typically, the state-of-the-art $\text{CO}_2/\text{C}_2\text{H}_2$ dynamic selectivity of 48.0 with high CO_2 dynamic uptake of 0.96 mmol/g can be achieved in the separation of $\text{CO}_2\text{-C}_2\text{H}_2\text{-He}$ mixture (5/10/85; v/v/v) under optimized conditions. The fine structure of Sr/K-HEU with the precise positioning of extraframework cations is identified by means of three-dimensional electron diffraction (3D ED). The interaction between guest molecules (CO_2 and C_2H_2) and gate-keeping cations (K^+ and Sr^{2+}) is investigated by theoretical simulations, showing a full picture of molecular trapdoor in inverse $\text{CO}_2\text{-C}_2\text{H}_2$ separation by Sr/K-HEU zeolite. This study not only provides a new example of trapdoor effect in zeolites for a challenging adsorptive separation process, but also improves our understanding on the underlying mechanism of molecular trapdoor.

Results and Discussion

HEU zeolite boasts a distinctive two-dimensional (2D) microporous channel system, characterized by two parallel channels comprised of 10-membered rings (channel A) and 8-membered rings (channel B), intersected by additional 8-membered rings (channel C), ultimately culminating in a layered architectural configuration.^[46] Commercial K-HEU zeolite ($\text{Si}/\text{Al}=3.9$) exhibits considerable adsorption capacities for both CO_2 and C_2H_2 (2.48 and 2.05 mmol/g for CO_2 and C_2H_2 , respectively, Figure 1a). The microporous surface area of K-HEU calculated from Ar adsorption-desorption isotherms at 87K is close to zero, demonstrating that Ar molecules cannot diffuse into the pores of zeolite (Supporting Information, Figure S1, Table S2). The great difference

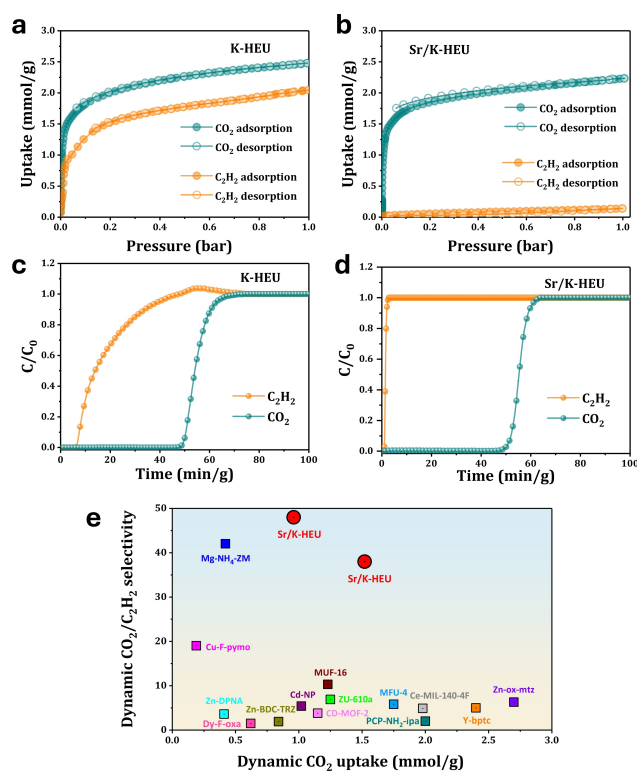


Figure 1. Adsorption isotherms of C_2H_2 and CO_2 on K-HEU (a) and Sr/K-HEU (b) at 298 K; Column breakthrough curves of $\text{CO}_2/\text{C}_2\text{H}_2/\text{He}$ (5/10/85, v/v/v; total gas flow: 8.5 mL/min) over a fixed-bed reactor packed with K-HEU (c) and Sr/K-HEU (d) at 298 K; (e) Plots of $\text{CO}_2/\text{C}_2\text{H}_2$ dynamic selectivity against dynamic CO_2 uptake under ambient conditions with representative adsorbents.

in the sorption performance of K-HEU zeolite toward molecules with similar kinetic diameters (3.4 Å for Ar and 3.3 Å for CO_2) implies that K-HEU might selectively open the door for CO_2 molecules, following the so-called trapdoor effect.^[44,45] Unfortunately, K-HEU exhibits molecular trapdoor effect for both C_2H_2 and CO_2 , resulting in poor separation ability. It is known that the interaction between extraframework cations and gas molecules plays a pivotal role in the observed molecular trapdoor effect, and thereby, it should be possible to achieve specific recognition of CO_2 via molecular trapdoor effect for $\text{CO}_2\text{-C}_2\text{H}_2$ separation simply by regulating the extraframework cations.

A series of alkaline-earth metal ion-exchanged M-HEU [$\text{M}=\text{Mg}(\text{II}), \text{Sr}(\text{II}), \text{Ba}(\text{II})$, with residual $\text{K}(\text{I})$] zeolites were prepared for $\text{CO}_2\text{-C}_2\text{H}_2$ adsorption and separation {due to the severe collapse of Ca/K-HEU framework during calcination process (Supporting Information, Figure S2, S9 and S10)^[47–49], it is not included in this study}. The XRD patterns, SEM images and Ar sorption isotherms of obtained zeolite samples are shown in Figure S1, S3–S4 (Supporting Information). Typically, M-HEU zeolites exhibit similar Ar sorption characteristics as K-HEU, and therefore, their microporous properties were determined by CO_2 sorption isotherms at 196K (Supporting Information, Table S2). M-HEU zeolites achieve high exchange degrees of >80% after three consecutive ion-exchange processes (Supporting Informa-

tion, Table S2), consistent with previous reports.^[50] The CO₂ and C₂H₂ sorption isotherms of M-HEU zeolites were measured at 298 K and 1 bar (Figure 1a–b, Supporting Information, Figure S5–S6). The saturated CO₂ adsorption capacities of M-HEU zeolites align closely with their micropore surface areas (Supporting Information, Figure S1, Table S2). In this context, regulating the extraframework cations of HEU zeolites to exclude C₂H₂ molecules becomes a feasible strategy to achieve one-step CO₂-C₂H₂ separation. As expected, the adsorption capacities of C₂H₂ display significant variations across various cations (Ba/K-HEU > K-HEU > Mg/K-HEU ≫ Sr/K-HEU), indicating a close correlation between the ability of C₂H₂ molecules to penetrate the structure and the presence of gate-keeping extraframework cations. Remarkably, Sr/K-HEU maintains a substantial uptake of CO₂ (2.21 mmol/g) while demonstrating only minimal uptake of C₂H₂ (0.14 mmol/g) at 298 K and 1 bar. Sr/K-HEU exhibits a noteworthy CO₂/C₂H₂ saturated uptake ratio of 15.8, surpassing that of known CO₂-selective adsorbents such as Cu-F-pymo (11.9),^[26] MUF-16 (11.9 at 293 K),^[28] Cd-NP (6.02),^[29] Mg-NH₄-ZM (6.2),^[30] Zn-ox-mtz (12.8),^[31] and Ce^{IV}-MIL-140-4F (2.7)^[32] (Supporting Information, Table S3). It underscores the potential of Sr/K-HEU zeolite as a low-cost adsorbent for CO₂-C₂H₂ separation due to the gate-keeping function of Sr²⁺, which selectively permits the passage of CO₂ molecules while hindering that of C₂H₂ (*vide infra*).

To assess the practical viability of M-HEU for CO₂-C₂H₂ separation, column breakthrough experiments for CO₂/C₂H₂/He mixture (5/10/85; v/v/v) were conducted at 298 K (Figure 1c–d, Supporting Information, Figure S7–S8). In consistent with static uptake results, all M-HEU zeolites exhibit earlier breakthrough of C₂H₂ than CO₂, and almost pure C₂H₂ (determined by the mass spectrum detection limit of 1 ppm) can be obtained prior to the breakthrough of CO₂, for example 45 min for Sr/K-HEU. The dynamic adsorption capacities of CO₂ for K-HEU, Mg/K-HEU, Sr/K-HEU and Ba/K-HEU are measured as 0.95, 0.66, 0.96 and 0.88 mmol/g, respectively. Accordingly, the dynamic separation selectivity of CO₂/C₂H₂ is determined as 3.1, 4.9, 48.0 and 2.5, respectively. Remarkably, the dynamic selectivity of Sr/K-HEU surpasses all known CO₂-selective adsorbents, including prominent MOFs, for instance, Cu-F-pymo (19.0),^[26] MUF-16 (10.3),^[28] Cd-NP (5.4),^[29] Mg-NH₄-ZM (42.0),^[30] Ce^{IV}-MIL-140-4F (4.9)^[32] and Y-bptc (33.0)^[23] (Supporting Information, Table S3). A comparison of experimentally-determined CO₂/C₂H₂ dynamic selectivity against dynamic CO₂ uptake further underscores the unprecedented performance of Sr/K-HEU in CO₂-C₂H₂ separation (Figure 1e). Sr/K-HEU appears to be the most selective adsorbent for inverse CO₂-C₂H₂ separation with sustainable CO₂ dynamic uptake. To our knowledge, Sr/K-HEU is the first eligible zeolite adsorbent for inverse CO₂-C₂H₂ separation. The impacts of operating conditions on CO₂-C₂H₂ separation on Sr/K-HEU were further investigated. The dynamic CO₂ uptake and CO₂/C₂H₂ selectivity keeps nearly unchanged with increasing gas flow rate from 8.5 to 20 mL/min, and the dynamic CO₂ uptake only shows a slight decrease with increasing temperature from 298 to 333 K

(Supporting Information, Figure S11–S15). Especially, the dynamic CO₂ uptake at 298 K increases to 1.52 mmol/g while the dynamic C₂H₂ uptake keeps unchanged at 0.04 mmol/g in high-concentration CO₂-C₂H₂ mixture (50/50; v/v) (Supporting Information, Figure S16). These results demonstrate the feasibility of Sr/K-HEU zeolite adsorbent for practical applications.

Temperature-programmed desorption (TPD) experiments were conducted to assess the adsorption strength and the recyclability of adsorbents. In a typical procedure, the zeolite adsorbent underwent initial dosing with a gas mixture of CO₂-C₂H₂ at 298 K, followed by primary Ar purging at the same temperature. Subsequently, TPD profiles of C₂H₂ and CO₂ were recorded in the temperature range of 298 to 650 K under flowing Ar. In principle, weakly adsorbed C₂H₂ and CO₂ molecules on adsorbents can be swiftly removed during the primary purging process, while the strongly adsorbed species are trapped in the adsorbents. As shown in Figure 2a, very weak C₂H₂ desorption peaks can be observed in the C₂H₂-TPD profile of Sr/K-HEU, indicating that trace weakly adsorbed C₂H₂ molecules on Sr/K-HEU are eliminated during the primary purging process. In contrast, distinct multiple C₂H₂ desorption peaks are observed in the temperature range of 323–500 K for Mg/K-HEU, Ba/K-HEU and K-HEU, in consistency with the results from static adsorption and dynamic breakthrough experiments. On the other hand, all M-HEU zeolites show

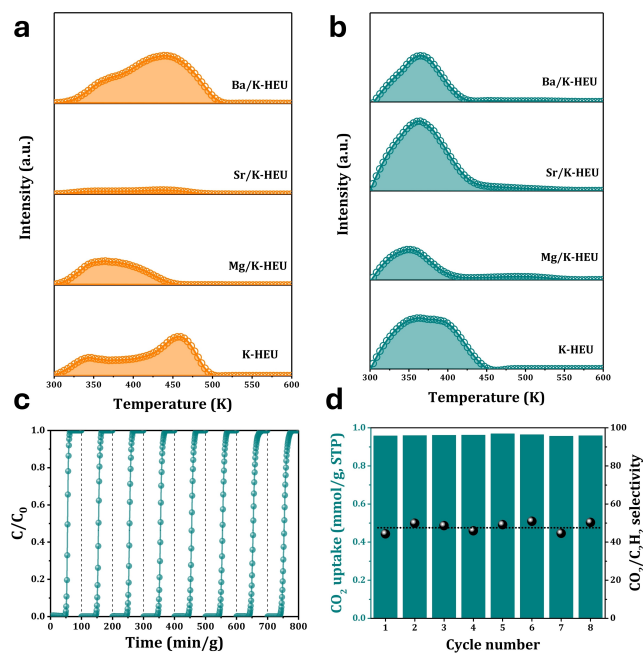


Figure 2. TPD profiles of (a) C₂H₂ and (b) CO₂ on M-HEU zeolites after saturated adsorption. Recycling performance of Sr/K-HEU at 298 K and 1 bar with a gas mixture of CO₂/C₂H₂/He (5/10/85, v/v/v) and total flow rate of 8.5 mL/min: (c) Recyclability of Sr/K-HEU in C₂H₂/CO₂ separation for eight cycles (only the CO₂ concentration curves are shown for conciseness); (d) Dynamic adsorption capacities of CO₂ and dynamic selectivity of CO₂/C₂H₂ in eight cycles. The saturated adsorbent was regenerated by heating at 473 K in flowing Ar for 30 minutes to remove adsorbed CO₂ between cycles.

distinct CO₂ desorption peaks in the temperature range of 298–453 K and Sr/K-HEU shows the largest CO₂ desorption peak among all samples under study (Figure 2b). According to the TPD profiles, the complete regeneration of M-HEU adsorbents can be achieved upon thermal treatment at 453 K or higher. As expected, the optimized Sr/K-HEU adsorbent shows perfect recyclability in eight continuous cycles of binary breakthrough experiments (Figure 2c). The dynamic CO₂ uptake (average: 0.96 mmol/g) and the CO₂-C₂H₂ selectivity (average: 47.8) can be well maintained in the recycling breakthrough tests (Figure 2d). These results highlight the straightforward temperature-swing adsorption process for CO₂-C₂H₂ separation employing Sr/K-HEU as a low-cost zeolite adsorbent (~\$2000 per ton).

To validate the adsorption affinity between CO₂ and M-HEU, the isosteric heats of adsorption (Q_{st}) of CO₂ within these zeolites were determined *via* TG-DSC measurements (Supporting Information, Figure S17–S20). The Q_{st} values obtained for M-HEU are 23.9, 28.2, 29.3 and 30.0 kJ/mol for Mg/K-HEU, Sr/K-HEU, K-HEU and Ba/K-HEU, respectively. All M-HEU zeolites exhibit desirable adsorption heat values of 30 kJ/mol at most, indicating the nature of physisorption. For the optimized adsorbent Sr/K-HEU, the isosteric heat was also calculated using the Clausius-Clapeyron equation from the isotherms measured across a range of temperatures (Supporting Information, Figure S21). The isosteric heat value of ~30 kJ/mol can be obtained (Supporting Information, Figure S22), in consistency with

that measured by TG-DSC. The data of isosteric heat further validate the good recyclability of Sr/K-HEU for CO₂-C₂H₂ separation.

Upon scrutiny of the empirical findings delineated above, it is rational to propose that the inverse CO₂-C₂H₂ separation is achieved by the trapdoor effect of extraframework cations in M-HEU zeolites, with delicate interplay between the guest molecules and the gate-keeping cations. The underlying mechanism in the molecular level is then explored, starting from the precise identification of extraframework cations in HEU zeolite. 3D ED technique was performed to unveil the crystallographic structure of Sr/K-HEU ($|\text{Sr}_{10}\text{K}_2|[\text{Al}_{22}\text{Si}_{86}\text{O}_{216}]$) and the location of extraframework cations. The high-quality 3D ED data (resolution 0.8 Å) was collected within 3 min (Supporting Information, Table S4). The possible space group ($C2$, Cm , and $C2/m$) can be deduced from reflection conditions of the reconstructed 3D reciprocal lattice (Supporting Information, Figure S23). The initial structure of Sr/K-HEU was solved by SHELXT^[51] with the space group of $C2/m$ and unit cell parameters of $a=17.0$ Å, $b=17.4$ Å, $c=7.4$ Å, $\alpha=90^\circ$, $\beta=113.9^\circ$, and $\gamma=90^\circ$. The locations of extraframework cations were identified by subsequent refinement *via* SHELXL.^[51] Conclusively, the architectural framework of Sr/K-HEU contains a 2D channel system, wherein 10MRs and 8MRs course along the [001] axis, denoted as channels A and B, respectively (Figure 3a). Channel C comprises 8MRs aligned along [100] (Figure 3d), and it is dense without pores along

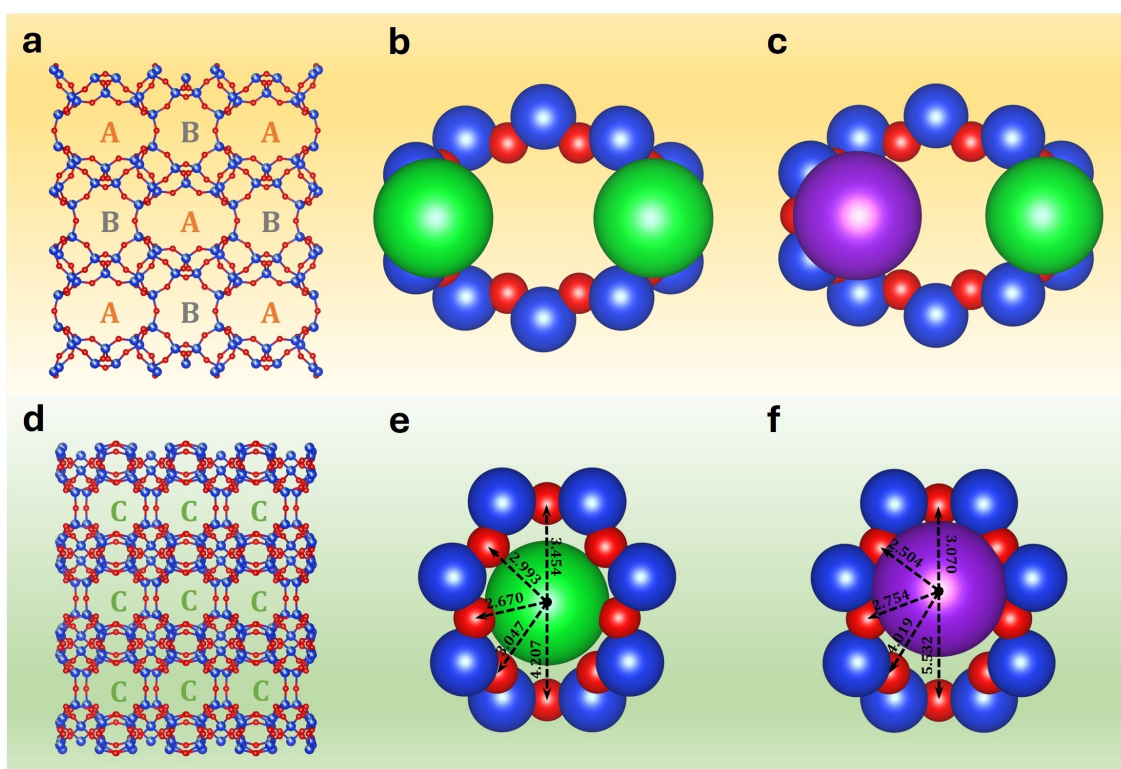


Figure 3. Views of framework structure and cation sites of Sr/K-HEU determined from 3D ED. The 10MRs and 8MRs run along [001] as channel A and channel B, respectively (a), and the 8MRs run along [100] as channel C (d). The extra-framework cations are located in the 10MR of channel A as 10MR-Sr/Sr (b) and 10MR-K/Sr (c), while occupying channel C as Sr²⁺ (e) and K⁺ (f). Si/Al: blue; O: red; Sr: green; K: purple.

the [010] direction, a configuration consistent with previous reports.^[52–54] Extra-framework cations, including Sr^{2+} and un-exchanged residual K^+ , stake their claim within 10MRs of channel A (Figure 3b–c) and also pervade 8MRs of channel C coordinating with framework oxygen atoms (closest Sr–O distance: 2.670 Å, closest K–O distance: 2.504 Å) (Figure 3e–f). It should be noted that, in consistent with the proportional distribution of cations, the 10MRs within channel A may be settled by double Sr^{2+} cations (Figure 3b) or Sr^{2+} - K^+ pairs (Supporting Information, Figure S24, Figure 3c).

In light of the complete blockage of the 8MRs within the channel C of Sr/K-HEU (Figure 3e–f), the possibility of molecules adsorption in the channel C can be fully ruled out. By analyzing the apparent difference between the properties of Ba/K-HEU and Sr/K-HEU, it can be concluded that the adsorption difference should not originate from the similar parts of the two zeolites (fully exposed 8MRs), but should come from the different parts, namely the 10MRs sheltered by different cations. The density distribution results also indicate that under the premise of guest molecule (CO_2 and C_2H_2) admission into internal cavities (Supporting Information, Figure S25), the molecules are only distributed along the channel A, so it is established from theoretical calculations that the 10MRs of channel A represent the sole pragmatic conduits for gas diffusion into the internal cavities. This revelation prompts an inquiry into the mechanism for the admission of guest molecules despite the apparent occlusion of the pore entrance in Sr/K-HEU. The only possibility is the robust interaction between guest molecules and the gate-keeping cations, which triggers a transient and reversible cation deviation, thus facilitating the entry of specific guest molecules into the internal cavities through the door of 10MRs. That is, the concept denoted as the “trapdoor” effect in previous reports.^[44,45,55] To unravel

the complexity of the guest admission process by the 10MRs of Sr/K-HEU, DFT calculations were performed to demonstrate the relative energy level for guest molecules to navigate past the gate-keeping cations. The initial state energy of the guest molecules prior to their approach to the 10MRs is set at 0 kJ/mol. The consequential energy differential, denoted as ΔE , represents the augmentation in energy level with the presence of guest molecules relative to the initial state energy. The snapshots capturing the adsorption configurations and trajectories of guest molecules and gate-keeping cations within the confined space of the 10MRs of Sr/K-HEU were investigated in detail. Both K^+ and Sr^{2+} are considered as the gate-keeping cations considering their co-presence in Sr/K-HEU (17% K^+ and 83% Sr^{2+}). The calculation model is based on the 3D ED resolved structure and the ratio of $\text{K}^+/\text{Sr}^{2+}$.

The interaction between CO_2 and K^+ from the 10MRs settled by Sr^{2+} - K^+ pairs (denoted as 10MR-K/Sr) was studied first. Typically, the interaction between CO_2 and K^+ initiates first a pivotal repositioning of the latter towards the center of the ring, effectuating complete occlusion (a transitional state mandating an energy barrier of 57 kJ/mol), then towards the periphery of the ring, transiently unblocking door of the 10MRs (a migration state necessitating an energy barrier of 36 kJ/mol), facilitating unimpeded passage of CO_2 . Subsequently, as CO_2 traverses further into the internal cavities, K^+ promptly reverts to its initial position to lock the door, thereby attaining the energy nadir of the system (Figure 4a). For the interaction between CO_2 and Sr^{2+} from the 10MRs settled by Sr^{2+} - K^+ pairs, similar dynamics could be observed. Briefly, the interaction between CO_2 and Sr^{2+} first initiates a subtle shift of Sr^{2+} towards the center of the ring (a transition state demanding an energy barrier of 44 kJ/mol), followed by a deviation towards the periphery to unblock the door of 10MRs (with

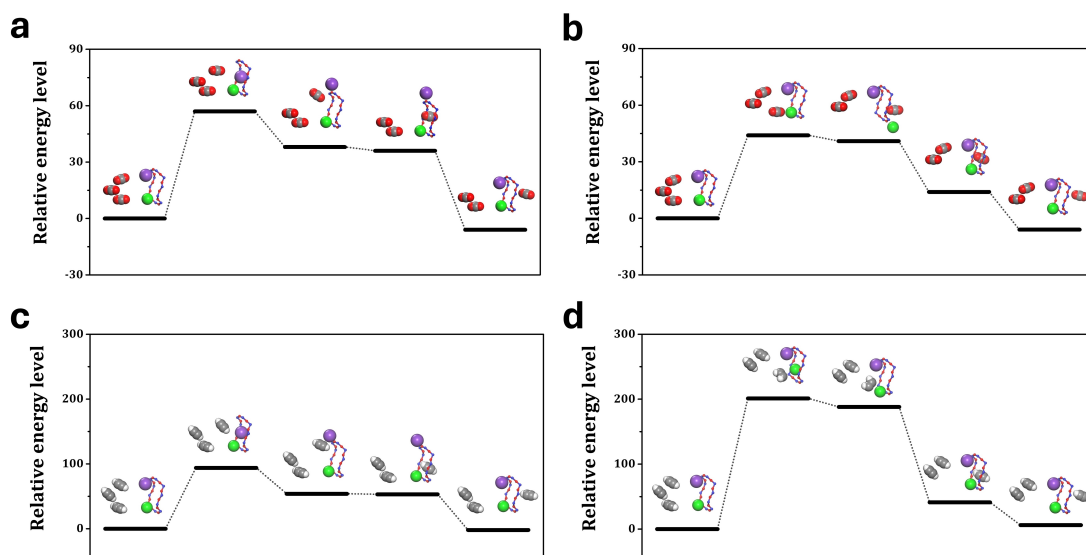


Figure 4. Illustration of the molecular trapdoor mechanism and the corresponding energy levels calculated by DFT. (a) The interaction between CO_2 and K^+ when passing through 10MR-K/Sr. (b) The interaction between CO_2 and Sr^{2+} when passing through 10MR-K/Sr. (c) The interaction between C_2H_2 and K^+ when passing through 10MR-K/Sr. (d) The interaction between C_2H_2 and Sr^{2+} when passing through 10MR-K/Sr.

an energy barrier of 41 kJ/mol). Notably, Sr^{2+} exhibits a transient affinity towards CO_2 during the homing process, underscoring the intricate host-guest dynamics (Figure 4b). According to the simulation results, CO_2 can pass through the door of 10MRs settled by Sr^{2+} - K^+ pairs with a low energy barrier of 44 kJ/mol (preferential interaction with Sr^{2+}). Interestingly, CO_2 can easily pass through the door of 10MRs settled by double Sr^{2+} cations (10MR-Sr/Sr) with exactly the same energy barrier of 44 kJ/mol (Supporting Information, Figure S28). That is, CO_2 molecules can diffuse into the internal cavities of HEU zeolite for adsorption by passing through the door of 10MRs, driven by the robust interaction between CO_2 and the dooring-keeping Sr^{2+} cation.

Upon the proximity of C_2H_2 to the 10MR-K/Sr, the interplay between C_2H_2 and K^+ was first considered with a trajectory mirroring that of CO_2 , namely the migration of K^+ towards the center of the ring before veering towards the periphery. However, both the transition and migration states necessitate high energy barriers, registering at 94 kJ/mol and 54 kJ/mol, respectively (Figure 4c). Considering the interaction between C_2H_2 and Sr^{2+} in 10MR-K/Sr, the subtle relocation of Sr^{2+} towards the center of the ring and subsequent migration towards the periphery necessitate a formidable energy barrier of 201 kJ/mol and 188 kJ/mol, respectively. The approaching C_2H_2 molecules undergo structure deformation owing to the strong repulsion from the positive charge towards the positive center of the molecule (H atom), making this mission impossible (Figure 4d). Similarly, it is impossible for C_2H_2 molecules to pass through the doors of 10MR-Sr/Sr (energy barriers >200 kJ/mol, Supporting Information, Figure S29). DFT simulation results reveal the vital role of extraframework cations on the inverse CO_2 - C_2H_2 separation by constructing trapdoor for molecular recognition, namely the molecular trapdoor. Specifically, C_2H_2 molecules cannot pass through the doors of 10MRs with Sr^{2+} as the gate-keeping cations, while they might be able to diffuse into the internal cavities through the doors of 10MRs upon the transient migration of gate-keeping K^+ (even though with high energy barriers). In this context, more residual K^+ as the gate-keeping cations should correspond to higher amount of C_2H_2 molecules adsorbed by Sr/K-HEU zeolite, as confirmed by the static C_2H_2 sorption isotherms (Supporting Information, Figure S30). If Sr-HEU zeolite free of residual K^+ could be prepared, perfect $\text{CO}_2/\text{C}_2\text{H}_2$ selectivity can be expected in both static adsorption isotherms and dynamic breakthrough experiments. In addition, we have to clarify that it is difficult to use only simulations to treat such a complicated system. However, with the combination of experimental observations and theoretical simulations, new insight into the molecular trapdoor effect can be gained.

Conclusion

The separation of CO_2 and C_2H_2 is an essential process to produce high-quality C_2H_2 for industrial applications, which faces formidable challenges posed by the almost identical

physical properties of the two molecules. We report herein the first example of zeolite adsorbent, namely Sr/K-HEU, for inverse CO_2 - C_2H_2 separation utilizing the molecular trapdoor effect. Experimentally, Sr/K-HEU shows unprecedented dynamic $\text{CO}_2/\text{C}_2\text{H}_2$ selectivity of 48.0, sustainable dynamic CO_2 uptake of 0.96 mmol/g and perfect recyclability in CO_2 - C_2H_2 separation, demonstrating its great potential for practical applications via a straightforward temperature-swing adsorption process.

The precise structure of Sr/K-HEU has been identified by 3D ED, showing 10MRs within channel A of HEU zeolite settled by Sr^{2+} - K^+ pairs or double Sr^{2+} as the gate-keeping cations. The interplay between the guest molecules (CO_2 or C_2H_2) and the gate-keeping cations (Sr^{2+} or K^+) has been investigated by DFT calculations. Typically, CO_2 can easily pass through the 10MRs of HEU zeolite upon the temporary and reversible deviation of gate-keeping cations while C_2H_2 cannot, thereby realizing the inverse CO_2 - C_2H_2 separation through the molecular trapdoor mechanism. Overall, an example of molecular trapdoor in Sr/K-HEU zeolite is demonstrated for the inverse CO_2 - C_2H_2 separation with the underlying mechanism well interpreted, providing new thoughts for separation by zeolites.

Acknowledgements

This work was supported by the National Natural Science Fund of China (22025203, 22302100 and 22102177), the Fundamental Research Funds for the Central Universities (Nankai University), the China Postdoctoral Science Foundation (2024T170439).

Conflict of Interest

The authors declare no conflict of interest.

Keywords: molecular trapdoor · HEU zeolite · CO_2 - C_2H_2 inverse separation · extra-framework cations

- [1] P. Pässler, W. Hefner, K. Buckl, H. Meinass, A. Meiswinkel, H. J. Wernicke, G. Ebersberg, R. Müller, J. Bässler, H. Behringer, *Acetylene in Ullmann's Encyclopedia of Industrial Chemistry*, Vol. 1, Weinheim: Wiley-VCH Verlag GmbH & Co. KGaA, **2012**, pp. 277–326.
- [2] R. Matsuda, R. Kitaura, S. Kitagawa, Y. Kubota, R. V. Belosludov, T. C. Kobayashi, H. Sakamoto, T. Chiba, M. Takata, Y. Kawazoe, Y. Mita, *Nature* **2005**, 436, 238.
- [3] I. T. Trotsuş, T. Zimmermann, F. Schüth, *Chem. Rev.* **2014**, 114, 1761.
- [4] J. R. Li, R. J. Kuppler, H. C. Zhou, *Chem. Soc. Rev.* **2009**, 38, 1477.
- [5] J. Pei, K. Shao, J. X. Wang, H. M. Wen, Y. Yang, Y. Cui, R. Krishna, B. Li, G. Qian, *Adv. Mater.* **2020**, 32, 1908275.
- [6] L. Z. Cai, Z. Z. Yao, S. J. Lin, M. S. Wang, G. C. Guo, *Angew. Chem. Int. Ed.* **2021**, 60, 18223.
- [7] L. Zhang, K. Jiang, L. Yang, L. Li, E. Hu, L. Yang, K. Shao, H. Xing, Y. Cui, Y. Yang, B. Li, B. Chen, G. Qian, *Angew. Chem. Int. Ed.* **2021**, 60, 15995.

- [8] R. B. Lin, S. Xiang, W. Zhou, B. Chen, *Chem* **2020**, *6*, 337.
- [9] J. Li, P. M. Bhatt, J. Li, M. Eddaoudi, Y. Liu, *Adv. Mater.* **2020**, *32*, 2002563.
- [10] Z. Di, C. Liu, J. Pang, C. Chen, F. Hu, D. Yuan, M. Wu, M. Hong, *Angew. Chem. Int. Ed.* **2021**, *60*, 10828.
- [11] Y. Yang, H. Zhang, Z. Yuan, J. Q. Wang, F. Xiang, L. Chen, F. Wei, S. Xiang, B. Chen, Z. Zhang, *Angew. Chem. Int. Ed.* **2022**, *61*, e202207579.
- [12] Z. Niu, X. Cui, T. Pham, G. Verma, P. C. Lan, C. Shan, H. Xing, K. A. Forrest, S. Suepaul, B. Space, A. Nafady, A. M. Al-Enizi, S. Ma, *Angew. Chem. Int. Ed.* **2021**, *60*, 5283.
- [13] L. Yang, L. Yan, Y. Wang, Z. Liu, J. He, Q. Fu, D. Liu, X. Gu, P. Dai, L. Li, X. Zhao, *Angew. Chem. Int. Ed.* **2021**, *60*, 4570.
- [14] Q. Dong, X. Zhang, S. Liu, R. B. Lin, Y. Guo, Y. Ma, A. Yonezu, R. Krishna, G. Liu, J. Duan, R. Matsuda, W. Jin, B. Chen, *Angew. Chem. Int. Ed.* **2020**, *59*, 22756.
- [15] Z. Zhang, C. Kang, S. B. Peh, D. Shi, F. Yang, Q. Liu, D. Zhao, *J. Am. Chem. Soc.* **2022**, *144*, 14992.
- [16] S. Chen, N. Behera, C. Yang, Q. Dong, B. Zheng, Y. Li, Q. Tang, Z. Wang, Y. Wang, J. Duan, *Nano Res.* **2021**, *14*, 546.
- [17] X. Zhang, R. B. Lin, H. Wu, Y. Huang, Y. Ye, J. Duan, W. Zhou, J. R. Li, B. Chen, *Chem. Eng. J.* **2022**, *431*, 134184.
- [18] H. Xu, Y. He, Z. Zhang, S. Xiang, J. Cai, Y. Cui, Y. Yang, G. Qian, B. Chen, *J. Mater. Chem. A* **2013**, *1*, 77.
- [19] Y. Belmabkhouta, Z. Zhang, K. Adila, P. M. Bhatta, A. Cadiua, V. Solovyeva, H. Xing, M. Eddaoudia, *Chem. Eng. J.* **2019**, *359*, 32.
- [20] W. Wang, G. D. Wang, B. Zhang, X. Y. Li, L. Hou, Q. Y. Yang, B. Liu, *Small* **2023**, *19*, 2302975.
- [21] Q. Liu, S. G. Cho, J. Hilliard, T.-Y. Wang, S.-C. Chien, L.-C. Lin, A. C. Co, C. R. Wade, *Angew. Chem. Int. Ed.* **2023**, *62*, e202218854.
- [22] B. K. Ling, M. Zeng, T. Zhang, J. W. Cao, R. Yang, L. Cheng, C. Y. Zhang, Y. Wang, K. J. Chen, *Chem. Commun.* **2023**, *59*, 10952.
- [23] C. He, P. Zhang, Y. Wang, Y. Zhang, T. Hu, L. Li, J. Li, *Sep. Purif. Technol.* **2023**, *304*, 122318.
- [24] D. S. Choi, D. W. Kim, D. W. Kang, M. Kang, Y. S. Chae, C. S. Hong, *J. Mater. Chem. A* **2021**, *9*, 21424.
- [25] L. Li, J. Wang, Z. Zhang, Q. Yang, Y. Yang, B. Su, Z. Bao, Q. Ren, *ACS Appl. Mater. Interfaces* **2019**, *11*, 2543.
- [26] Y. Shi, Y. Xie, H. Cui, Y. Ye, H. Wu, W. Zhou, H. Arman, R. B. Lin, B. Chen, *Adv. Mater.* **2021**, *33*, 2105880.
- [27] Y. Gu, J. Zheng, K. Otake, M. Shivanna, S. Sakaki, H. Yoshino, M. Ohba, S. Kawaguchi, Y. Wang, F. Li, S. Kitagawa, *Angew. Chem. Int. Ed.* **2021**, *60*, 11688.
- [28] O. T. Qazvini, R. Babarao, S. G. Telfer, *Nat. Commun.* **2021**, *12*, 197.
- [29] Y. Xie, H. Cui, H. Wu, R. B. Lin, W. Zhou, B. Chen, *Angew. Chem. Int. Ed.* **2021**, *60*, 9604.
- [30] B. Ma, D. Li, Q. Zhu, Y. Li, W. Ueda, Z. Zhang, *Angew. Chem. Int. Ed.* **2022**, *61*, e202209121.
- [31] S. Q. Yang, R. Krishna, H. Chen, L. Li, L. Zhou, Y. F. An, F. Y. Zhang, Q. Zhang, Y. H. Zhang, W. Li, T. L. Hu, X. H. Bu, *J. Am. Chem. Soc.* **2023**, *145*, 13901.
- [32] Z. Zhang, S. B. Peh, R. Krishna, C. Kang, K. Chai, Y. Wang, D. Shi, D. Zhao, *Angew. Chem. Int. Ed.* **2021**, *60*, 17198.
- [33] J. Cui, Z. Qiu, L. Yang, Z. Zhang, X. Cui, H. Xing, *Angew. Chem. Int. Ed.* **2022**, *61*, e202208756.
- [34] R. T. Yang, *Gas Separation by Adsorption Processes*, Butterworth, Stoneham, **1987**, pp. 9–48.
- [35] B. Yue, S. Liu, Y. Chai, G. Wu, N. Guan, L. Li, *J. Energy Chem.* **2022**, *71*, 288.
- [36] P. J. Bereciartua, Á. Cantín, A. Corma, J. L. Jordá, M. Palomino, F. Rey, S. Valencia, E. W. Corcoran, P. Kortunov, P. I. Ravikovitch, A. Burton, C. Yoon, Y. Wang, C. Paur, J. Guzman, A. R. Bishop, G. L. Casty, *Science* **2017**, *358*, 1068.
- [37] S. Liu, X. Han, Y. Chai, G. Wu, W. Li, J. Li, I. da Silva, P. Manuel, Y. Cheng, L. L. Daemen, A. J. Ramirez-Cuesta, W. Shi, N. Guan, S. Yang, L. Li, *Angew. Chem. Int. Ed.* **2021**, *60*, 6526.
- [38] J. P. Zhang, X. M. Chen, *J. Am. Chem. Soc.* **2008**, *130*, 6010.
- [39] D. D. Zhou, J. P. Zhang, *Acc. Chem. Res.* **2022**, *55*, 2966.
- [40] Q. Gao, J. Xu, D. Cao, Z. Chang, X. H. Bu, *Angew. Chem. Int. Ed.* **2016**, *55*, 15027.
- [41] C. Gu, N. Hosono, J. J. Zheng, Y. Sato, S. Kusaka, S. Sakaki, S. Kitagawa, *Science* **2019**, *363*, 387.
- [42] J. Shang, G. Li, R. Singh, P. Xiao, J. Z. Liu, P. A. Webley, *J. Phys. Chem. C* **2013**, *117*, 12841.
- [43] J. Shang, G. Li, Q. Gu, R. Singh, P. Xiao, J. Z. Liu, P. A. Webley, *Chem. Commun.* **2014**, *50*, 4544.
- [44] J. Shang, G. Li, R. Singh, Q. Gu, K. M. Nairn, T. J. Bastow, N. Medhekar, C. M. Doherty, A. J. Hill, J. Z. Liu, P. A. Webley, *J. Am. Chem. Soc.* **2012**, *134*, 19246.
- [45] J. Zhao, S. H. Mousavi, G. Xiao, A. H. Mokarizadeh, T. Moore, K. Chen, Q. Gu, R. Singh, A. Zavabeti, J. Z. Liu, P. A. Webley, G. K. Li, *J. Am. Chem. Soc.* **2021**, *143*, 15195.
- [46] M. W. Ackley, R. T. Yang, *Ind. Eng. Chem. Res.* **1991**, *30*, 2523.
- [47] G. Cruciani, *J. Phys. Chem. Solids* **2006**, *67*, 1973.
- [48] I. K. Butikova, Y. F. Shepelev, Y. I. Smolin, *Crystallogr. Rep.* **1993**, *38*, 461.
- [49] D. L. Bish, *Eur. J. Mineral* **1990**, *2*, 771.
- [50] R. T. Yang, *Adsorbents: Fundamentals and Applications*, John Wiley & Sons, Hoboken, **2004**, pp. 173–183.
- [51] G. M. Sheldrick, *Acta Cryst.* **2008**, *A64*, 112.
- [52] R. M. Kakhki, S. Zirjanizadeh, M. Mohammadpoor, *J. Mater. Sci.* **2023**, *58*, 10555.
- [53] D. A. Kennedy, F. H. Tezel, *Micropor. Mesopor. Mater.* **2018**, *262*, 235.
- [54] D. A. Kennedy, M. Khanafer, F. H. Tezel, *Micropor. Mesopor. Mater.* **2019**, *281*, 123.
- [55] X. Wang, N. Yan, M. Xie, P. Liu, P. Bai, H. Su, B. Wang, Y. Wang, L. Li, T. Cheng, P. Guo, W. Yan, J. Yu, *Chem. Sci.* **2021**, *12*, 8803.

Manuscript received: October 3, 2024

Revised manuscript received: November 26, 2024

Accepted manuscript online: November 26, 2024

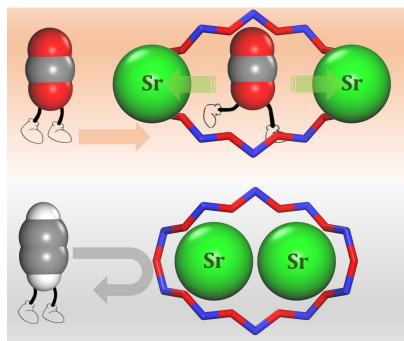
Version of record online: December 13, 2024

Research Article

Gas Separation

J. Jia, N. Yan, X. Lian, S. Liu,* B. Yue,
Y. Chai, G. Wu, J. Xu, L. Li* — e202419091

Molecular Trapdoor in HEU Zeolite Enables
Inverse CO₂-C₂H₂ Separation



Sr-exchanged K-type clinoptilolite (Sr/K-HEU) zeolite exhibits molecular trapdoor effect and thereby achieves inverse separation of CO₂-C₂H₂ with benchmark selectivity, which provides new thoughts for gas separation by zeolites and improves current understanding of molecular trapdoor mechanism.